


Article

Design and Experimental Verification of 400-W Class LED Driver with Cooperative Control Method for Two-Parallel Connected DC/DC Converters

Tomoharu Yada ¹, Yuta Katamoto ², Hiroaki Yamada ^{2,*}, Toshihiko Tanaka ², Masayuki Okamoto ³ and Tsuyoshi Hanamoto ⁴ 

¹ New Japan Radio Co., Ltd., 3-10, Nihonbashi Yokoyama-cho, Chuo-ku, Tokyo 103-8456, Japan; tyada@njr.co.jp

² Graduate School of Sciences and Technology for Innovation, Yamaguchi University, 2-16-1, Tokiwadai, Ube city, Yamaguchi 755-8611, Japan; v010vk@yamaguchi-u.ac.jp (Y.K.); totanaka@yamaguchi-u.ac.jp (T.T.)

³ Department of Electrical Engineering, National Institute of Technology, Ube College, 2-14-1, Tokiwadai, Ube city, Yamaguchi 755-8555, Japan; mokamoto@ube-k.ac.jp

⁴ Graduate School of Life Science and Systems Engineering, Kyushu Institute of Technology, 2-4, Hibikino, Wakamatsu, Kitakyushu city, Fukuoka 808-0196, Japan; hanamoto@life.kyutech.ac.jp

* Correspondence: hiro-ymd@yamaguchi-u.ac.jp; Tel.: +81-836-85-9471

Received: 26 July 2018; Accepted: 23 August 2018; Published: 26 August 2018



Abstract: This paper deals with a design and experimental verification of 400-W class light-emitting diode (LED) driver with cooperative control method for two-parallel connected DC/DC converters. In the cooperative control method, one DC/DC converter is selected to supply the output current for the LED, based on the reference value of the LED current. Thus, the proposed cooperative-control strategy achieves wide dimming range operation. The discontinuous current conduction mode (DCM) operation improves the total harmonic distortion (THD) value on the AC side of the LED driver. The standard of Electrical Applications and Materials Safety Act in Japan has defined the flicker frequency and minimum optical output. The smoothing capacitors are designed by considering the power flow and LED current ripple for satisfying the standard. A prototype LED driver is constructed and tested. Experimental results demonstrate that a wide dimming operation range from 1 to 100% is achieved with a THD value less than 10% on the AC side, by the proposed control strategy. The authors compare the power conversion efficiency between Si- and SiC-metal-oxide-semiconductor field-effect transistors (MOSFETs) based LED driver. The maximum power conversion efficiency by using SiC-MOSFETs based LED driver is 91.4%. Finally, the variable switching frequency method is proposed for improving the power conversion efficiency for a low LED current region.

Keywords: LED driver; wide dimming operation; single-stage; parallel-connected DC/DC converter topology; cooperative control

1. Introduction

The 21st Conference of the Parties (COP21) of the United Nations Framework Convention on Climate Change, in December 2015, offered to set in motion an ambitious cycle of improved climate and clean energy action [1]. The energy efficiencies of the industries, buildings and transport facilities must be increased. In the field of lighting fixtures, light-emitting diodes (LEDs) are widely used to reduce energy consumption. Moreover, since the adoption of the Minamata Convention on Mercury in October 2013 [2], LED floodlights have been superseding the mercury lamps. LEDs offer many advantages such as high luminance efficiency, long operating life and high-speed response for many applications [3]. Two-stage topology is the most popular topology for LED drivers above 100 W because

it provides a high power factor and low total harmonic distortion on the source side [4,5]. However, the power conversion efficiency is low because the converters are connected in series. To overcome this problem, single-stage forward and flyback power factor correction (PFC) converters with one active element [6], and single-stage half-bridge LLC DC-DC resonant converters [7,8] have been proposed. However, these topologies have complicated circuits and control algorithms. An efficient driver topology has been proposed in which a rectifier circuit with a diode bridge provides the forward voltage for the LED and the flyback converter controls the LED current [9]. This topology provides high efficiency at a low cost. However, for LED floodlights, this imposes limitations on the dimming range because the LED forward voltage is close to the rectified voltage of the diode rectifier circuit. Jane et al. have proposed a circuit topology with two parallel-connected flyback converters to overcome these limitations [10]. This single-stage topology uses two AC/DC converters with the outputs connected in series. One AC/DC converter provides the LED forward voltage, while the other AC/DC converter controls the LED current. The inputs of the two AC/DC converters are connected in parallel. Thus, the power conversion efficiency in the single-stage topology is an improvement over the two-stage topology, although it imposes a constraint on the minimum on-time of the active elements when the LED current is low. The authors have proposed a cooperative control method for the LED driver, using a parallel-connected flyback converter [11]. In this method, two DC/DC converters are controlled individually in response to the reference value of the LED current. However, the controller must be complex in order to achieve power factor correction (PFC) control because the proposed system has been designed in the critical conduction mode.

The authors have proposed a novel cooperative control method for an LED driver with a wide dimming range [12]. In this control method, two DC/DC converters are controlled individually in response to the reference value of the LED current. The two DC/DC converters are driven in the discontinuous mode (DCM). Therefore, the controller can achieve PFC in a simple manner, and the switching frequency is fixed. A lower current can be achieved, as compared to [11], by this proposed method. However, the design method for the smoothing capacitors wasn't discussed in [12]. In addition, the Si-metal-oxide-semiconductor field-effect transistors (MOSFETs) have been used for DC/DC converters in [12]. As a result, the maximum power conversion efficiency was 90.5%.

This paper deals with a design and experimental verification of 400-W class LED driver with a cooperative control method for two-parallel connected DC/DC converters. The standard of Electrical Applications and Materials Safety Act in Japan [13] has defined the flicker frequency and minimum optical output. The smoothing capacitors are designed by considering the power flow and LED current ripple for satisfying the standard. Digital computer simulations are performed using the PLECS software (Ver.4.1.8, Plexim, Zürich, Switzerland), to confirm the validity of the proposed method. A prototype LED driver is constructed and tested. The proposed LED driver reduces the minimum LED current by 90.7%, compared to the conventional control method. Experimental results demonstrate that a wide dimming operation, from 1% to 100%, can be achieved with a THD value less than 10% on the AC side, by the proposed control strategy. The linear dimming is confirmed by changing the reference LED current. From simulation and experimental results, the proposed LED driver can achieve stable operation. However, dynamic analysis is not conducted. In a future work, it would be important to examine the system for its stability. The maximum power conversion efficiency by using SiC-MOSFETs based LED driver is 91.4%. Finally, the variable switching frequency method is proposed for improving the power conversion efficiency for low LED current region.

The main contributions of this paper are as follows:

- Design of the smoothing capacitor for satisfying the standard of Electrical Applications and Materials Safety Act in Japan,
- Dynamic response of the proposed LED driver when the reference LED current is changed,
- Comparison of power conversion efficiency between Si- and SiC-MOSFETs,
- Improvement of power conversion efficiency in low current range by the proposed variable switching frequency method.

2. Conventional Control Method

In general, a high-brightness LED driver circuit of more than 150 W consists of two series-connected converters, which are a boost converter with a PFC controller and a DC/DC converter to control the LED current. However, the power conversion efficiency is poor.

To overcome this problem, Jane has proposed a circuit topology with two parallel-connected constant-voltage output converters and constant current output converters [10]. Figure 1 shows the power circuit diagram of the single-stage topology [11]. This single-stage topology has higher power conversion efficiency than the two-stage topology. As shown in Figures 2 and 3, one DC/DC converter provides the LED forward voltage, while another DC/DC converter controls the LED current. Moreover, both converters implement the PFC control. These two converters are connected in parallel at the input ports and in series at the output ports.

However, this topology cannot control low LED currents because of the constraint of minimum duty ratio. If the reference LED current is small, the output voltage of the DC/DC converter for LED current control must be small. In this particular case, the duty ratio of the DC/DC converter for LED current control must be small. This means that the turn-on time of the switching device must be less. Therefore, the switching device cannot control perfectly in this region.

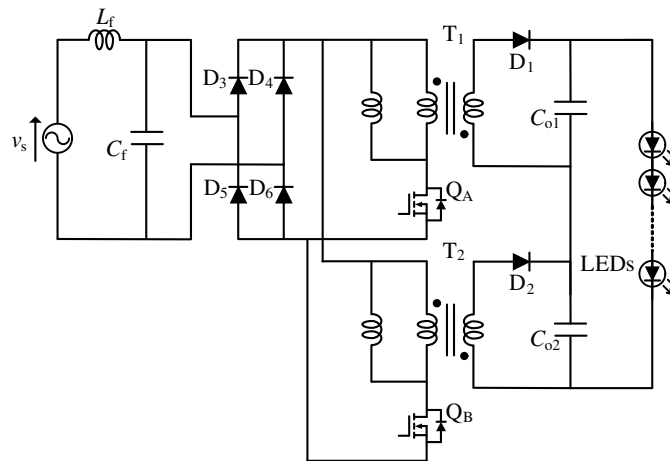


Figure 1. Previously proposed circuit diagram of light-emitting diode (LED) driver [4].

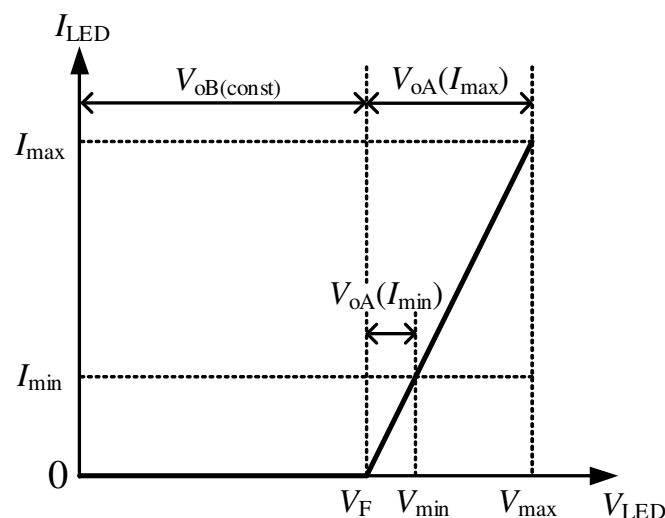


Figure 2. Output ranges of the converters with the conventional method.

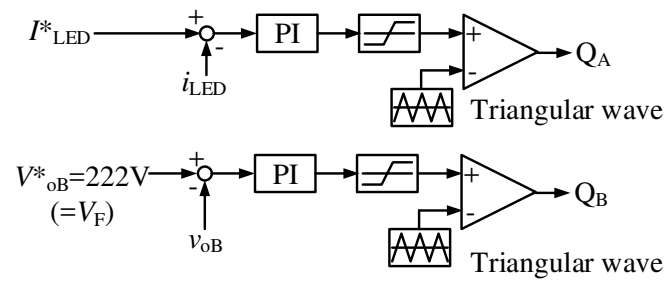


Figure 3. Control block of the proposed conventional method.

3. System Configuration

Figure 4 shows the power circuit diagram of the proposed LED driver. In this paper, we use an LED floodlight in which 72 LEDs are connected in series. The threshold voltage V_F is 222 V and the rated LED current is 1.5 A. At the rated output, the buck–boost chopper outputs the threshold voltage of the LED lamp. This circuit is equivalent to a constant-current source, and it can control the forward current of the LED accurately. This circuit can operate in the linear dimming mode. The buck–boost chopper is not galvanic isolation so the insulation is inferior to the conventional circuit. However, galvanic isolation is not necessarily required in LED applications. By using a non-insulated buck–boost chopper, the transformer is replaced with an inductor so that it can deal with larger electric power as compared with a transformer of the same volume, so it can be miniaturized.

By operating in DCM, it can improve the power supply power factor using a simpler control system compared to [11]. In the steady state of the buck–boost chopper, the magnetizing inductance of the buck–boost converter, L_1 , must satisfy the discontinuous current condition. The discontinuous current condition is given by

$$R_{LED} \geq \frac{2L_1 f_{sw}}{(1 - D_{QB})^2}, \quad (1)$$

where R_{LED} is the equivalent resistance of the LEDs, f_{sw} is the switching frequency, D_{QB} is the duty ratio of Q_B . From Equation (1), L_1 must be 63 μ H for achieving the rated output operation. Similarly, the discontinuous current condition for the flyback converter in the steady state is given by

$$D_{QA} \left(1 + \frac{nV_{Rec-max}}{V_{oA}}\right) \leq 1, \quad (2)$$

where D_{QA} is the duty ratio of Q_A . $V_{Rec-max}$ is the maximum value of the input voltage of both converters, and V_{oA} is the output voltage of the fly-back converter. From Equation (2), L_p is 228 μ H, $n = N_p/N_s$ is 9/24. The value of the smoothing capacitors C_{o1} and C_{o2} are decided by the acceptable current ripple of the LED as per the standard of Electrical Appliances and Materials Safety Act in Japan [13].

By [13], when the flicker frequency is 100 Hz or more and less than 500 Hz, the minimum optical output must be over 5% of the rated output. The flicker frequency of I_{LED} is twice the AC source frequency, which is 50 Hz or 60 Hz. Figure 5 shows the relationship between the LED current and LED illuminance. The blue dots are the measurement LED illuminance and the red line is the linear extrapolation. The LED illuminance shows saturation characteristics for the LED current. If we assume that the LED optical output is a linear function of I_{LED} , the actual flicker characteristics are better than the standard value, and the maximum LED current ($I_{LED-max}$) and the minimum LED current ($I_{LED-min}$) can be expressed by:

$$\frac{I_{LED-min}}{I_{LED-max}} > \alpha, \quad (3)$$

and, in this case, $\alpha = 0.05$. Figure 6 shows the relationship between the LED current and LED voltage ripples. ϵ_I and ϵ_V are the LED current and voltage ripples, respectively. $I_{LED-max}$ and $I_{LED-min}$ can be expressed by:

$$\begin{aligned} I_{LED-max} &= \frac{(1 + \epsilon_V) V_{DC} - V_F}{R_{LED}}, \\ I_{LED-min} &= \frac{(1 - \epsilon_V) V_{DC} - V_F}{R_{LED}}. \end{aligned} \quad (4)$$

From Equations (3) and (4), ϵ_V can be expressed by:

$$\epsilon_V = \frac{(1 - \alpha) (V_{DC} - V_F)}{(1 + \alpha) V_{DC}}. \quad (5)$$

Figure 7 shows the relationship between the power flows and voltage ripple of the smoothing capacitor. p_{in} is the input power of the smoothing capacitor and LED. p_{out} is the output power of the LED. p_c is the inflow and outflow power of the smoothing capacitor. When output power is at a maximum, the output voltage V_{DC} is 272 V and ϵ_V is the maximum value as 0.166. Assuming the power factor is 1, source voltage, current and input power can be expressed by:

$$\begin{aligned} v_s(t) &= \sqrt{2} V_{rms} \sin\left(2\pi \frac{t}{T_s}\right), \\ i_s(t) &= \sqrt{2} I_{rms} \sin\left(2\pi \frac{t}{T_s}\right), \\ p_{in}(t) &= 2P \sin^2\left(2\pi \frac{t}{T_s}\right), \end{aligned} \quad (6)$$

where T_s is the AC source voltage period and P is $V_{rms} I_{rms}$.

Assuming the power conversion efficiency is 100%, the power into and out of the smoothing capacitor ΔP_C can be expressed by:

$$\begin{aligned} \Delta P_C &= p_{in}(t) - P \\ &= 2P \sin^2\left(2\pi \frac{t}{T_s}\right) - P. \end{aligned} \quad (7)$$

In addition, the energy into the smoothing capacitor ΔU_{C-in} can be expressed by:

$$\begin{aligned} \Delta U_{C-in} &= \int_{t_0}^{t_0+T_s/4} \left[2P \sin^2\left(2\pi \frac{t}{T_s}\right) - P \right] dt \\ &= P \frac{T_s}{2\pi}. \end{aligned} \quad (8)$$

Otherwise, ΔU_{C-in} can be expressed with ϵ_V by:

$$\Delta U_{C-in} = \frac{1}{2} C_o \left[\{(1 + \epsilon_V) V_{DC}\}^2 - \{(1 - \epsilon_V) V_{DC}\}^2 \right], \quad (9)$$

where C_o is the combined smoothing capacitor of C_{o1} and C_{o2} . From Equations (8) and (9),

$$C_o = \frac{PT_s}{4\pi\epsilon_V V_{DC}^2}. \quad (10)$$

When the output power is the maximum as 408 W and T_s is 1/60 Hz, C_o is 44.06 μF . C_{o1} and C_{o2} are series connection. Therefore, C_o can be expressed by:

$$C_o = \frac{C_{o1}C_{o2}}{C_{o1} + C_{o2}}. \quad (11)$$

Thus, C_{o1} and C_{o2} are 110 μF in this paper. Table 1 indicates the circuit constants of the proposed LED driver.

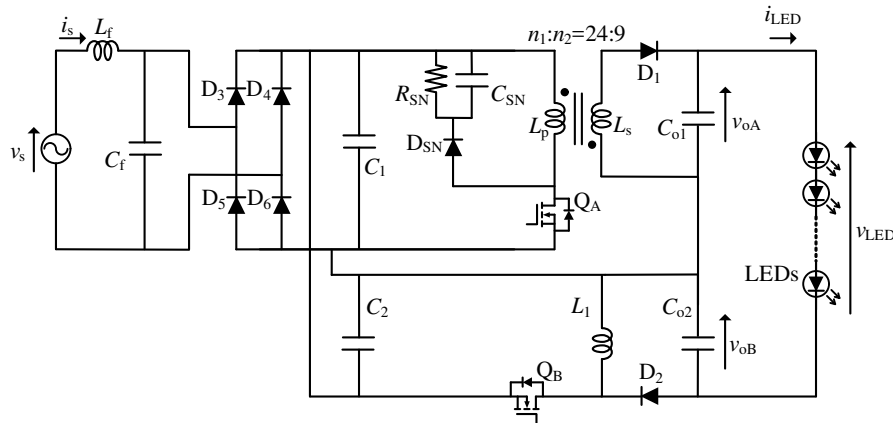


Figure 4. Power circuit diagram of the proposed LED driver.

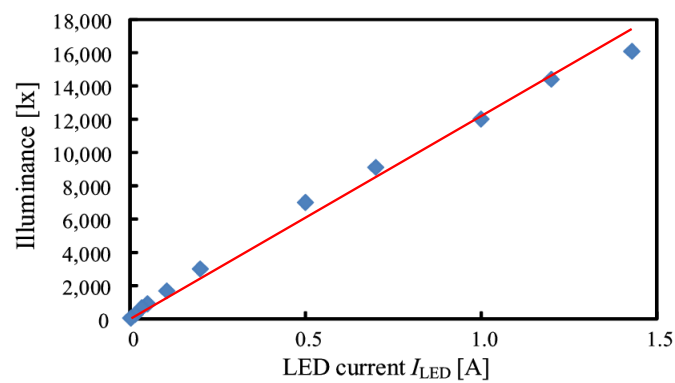


Figure 5. Relationship between the LED current and LED illuminance.

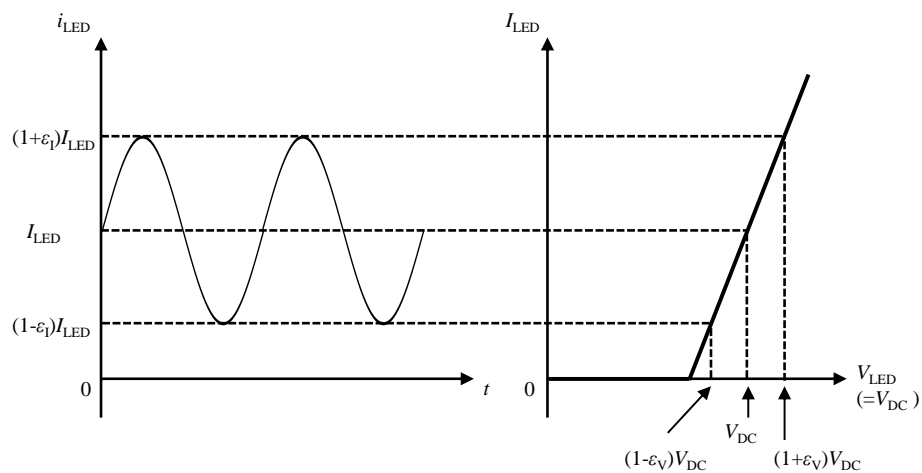


Figure 6. Relationship between the LED current and LED voltage ripples.

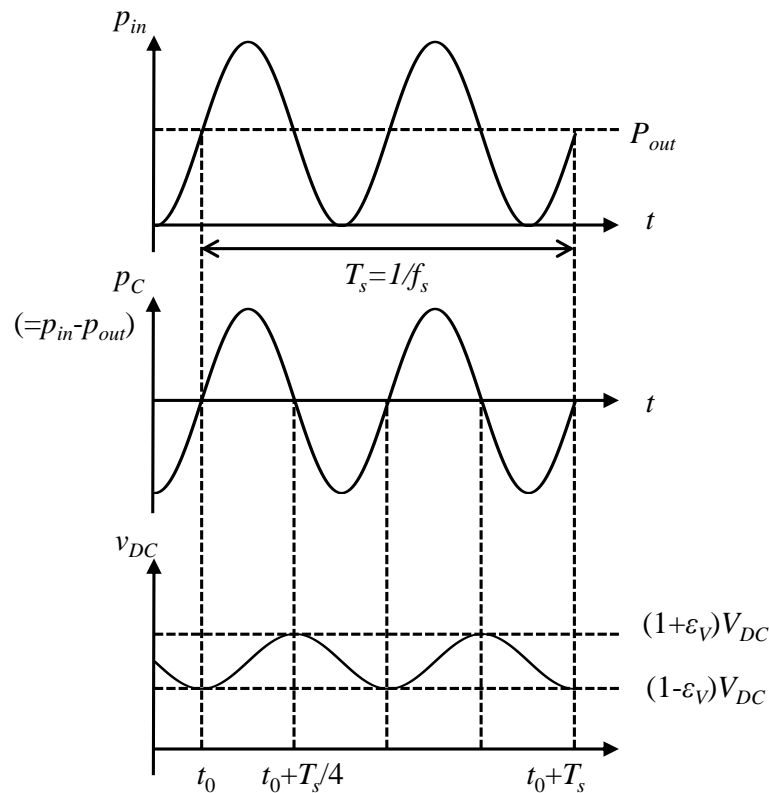


Figure 7. Relationship between the power flows and voltage ripple of the smoothing capacitor.

Table 1. Circuit constants of the proposed LED driver.

Item	Symbol	Value
AC source voltage	V_s	100 Vrms
Inductance of filter inductor	L_f	265 μ H
Capacitance of filter capacitor	C_f	0.1 μ F
Capacitance	C_1, C_2	0.1 μ F, 0.1 μ F
Capacitance	C_{o1}, C_{o2}	110 μ F, 110 μ F
Buck-boost inductance	L_1	69 μ H
Turn ratio	$N_1:N_2$	24:9
Inductance of primary side	L_p	228 μ H
Snubber resistance	R_{SN}	23.5 k Ω
Snubber Capacitance	C_{SN}	1 nF
Switching frequency	f_{sw}	50 kHz

4. Proposed Cooperative Control Method

The authors have proposed a cooperative control method for an LED driver with a wide a dimming range to overcome the technical issues of the conventional control method [11]. Figure 8 shows the output ranges of the converters with the proposed cooperative control method. In this control method, the output voltage V_{oB} of the buck–boost converter, which is used for voltage control, changes in response to the LED current. Therefore, Q_A can operate in the stable region. The proposed control method makes it possible for the LED driver to control LED currents as low as 15 mA.

The output voltages of the fly-back converter V_{oA} and the buck–boost chopper V_{oB} are given by

$$V_{oA} = T_{on(QA)} V_{Rec} \sqrt{\frac{\eta R_{LED} f_{sw}}{2L_p}}, \quad (12)$$

$$V_{oB} = V_{LED} - T_{on(QA)} V_{Rec} \sqrt{\frac{\eta R_{LED} f_{sw}}{2L_p}}, \quad (13)$$

where V_{LED} is the applied voltage of the LED and η is the power-conversion efficiency of the fly-back converter. In general, the on-interval of the switching device must be more than 10 times the turn-on time of the switching device, for stable gate driving. In this paper, we use the MOSFETs (STF20NM65N). From its data sheet, the minimum value of the on-time is determined to 300 ns. The minimum value of the LED current in the conventional control method is 161 mA under this condition.

It is assumed that the on interval $T_{on(QA)}$ is over 300 ns when the output current is 1% of the rated LED current. Under these conditions, the output voltage of the fly-back converter is determined to be $V_{oA} = 21.5$ V from Equation (13). Assuming $V_{oA} = 30$ V, the output voltage of the buck-boost chopper is determined as $V_{oB} = 197$ V from Equation (12). The reference value of the buck-boost converter V_{oB}^* changes in response to the reference value of I_{LED}^* . From Equation (13), the reference value V_{oB}^* is given as follows:

$$V_{oB}^*(I_{LED}^*) = 19.9I_{LED}^* + 192. \quad (14)$$

Figure 9 shows the control block of the proposed cooperative control method.

In this paper, the AC source voltage is 100 Vrms. From Equation (12), if the AC source voltage is higher, $T_{on(QA)}$ is under 300 ns when the output current is 1% of the rated LED current. When the AC source voltage is changed, the system parameters need to be redesigned.

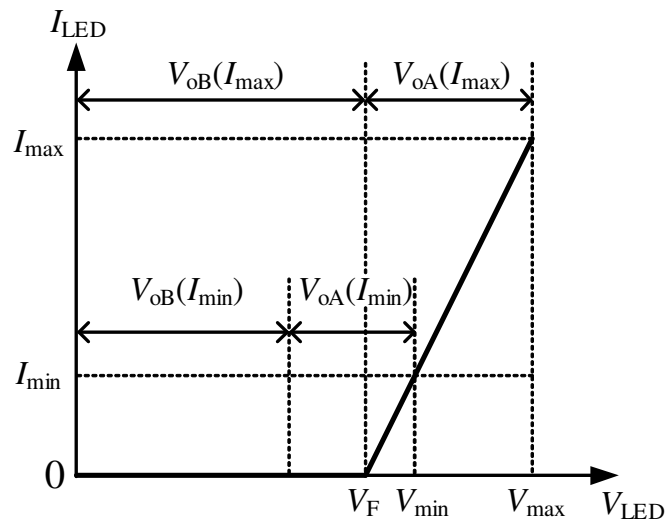


Figure 8. Output ranges of the converters with the proposed cooperative control method.

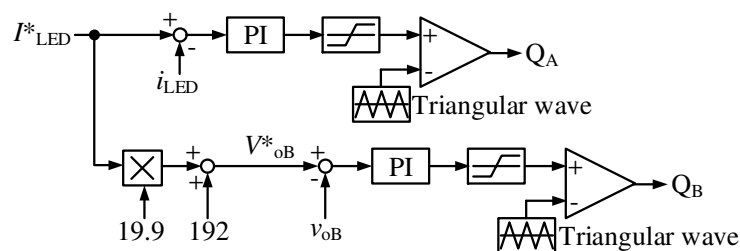


Figure 9. Control block of the proposed cooperative control method.

5. Simulation Results

Digital computer simulations were performed using the PLECS software, to confirm the validity of the proposed method. The LED floodlight, which was modeled by the linear diode, included the threshold voltage V_F and the on-resistance on the simulator.

Figure 10 shows the simulation results of the proposed cooperative control method when the reference LED current I_{LED}^* is 1.5 A. v_s is the source voltage, i_s is the source current, V_{oB} is the output voltage of the buck–boost chopper, and I_{LED} is the LED current. From Figure 10, it can be observed that the average LED current agrees with the reference LED current of 1.5 A. In addition, i_s is nearly sinusoidal and the power factor is 0.99.

Figure 11 shows the LED current and the output voltage of the buck–boost chopper for the reference output current I_{LED}^* . The solid line is the reference value V_{oB}^* calculated from Equation (14). In Figure 11, the red and blue dots represent the simulation results. From Figure 11, we can observe that the outputs of both converters agree with the reference values.

Figure 12 shows the simulation result of the transient response characteristic for the reference LED current I_{LED}^* . I_{LED}^* is changed from the minimum reference LED current 15 mA to the maximum 1.5 A in about 0.1 s. The output voltage of the buck–boost chopper V_{oB} and the output LED current are changed stably from the minimum value to the maximum in about 0.5 s.

Figures 13 and 14 show the Fast Fourier Transform (FFT) analysis results of i_s . From these figures, it can be inferred that the LED driver with the proposed cooperative control method can satisfy the conditions of IEC61000-3-2.

Figure 15 shows the simulated waveforms of the drain currents $i_{ds(QA)}$ and $i_{ds(QB)}$ for a reference LED current I_{LED}^* of 15 mA. From these waveforms, it can be observed that the on-intervals of Q_A and Q_B are always more than 300 ns.

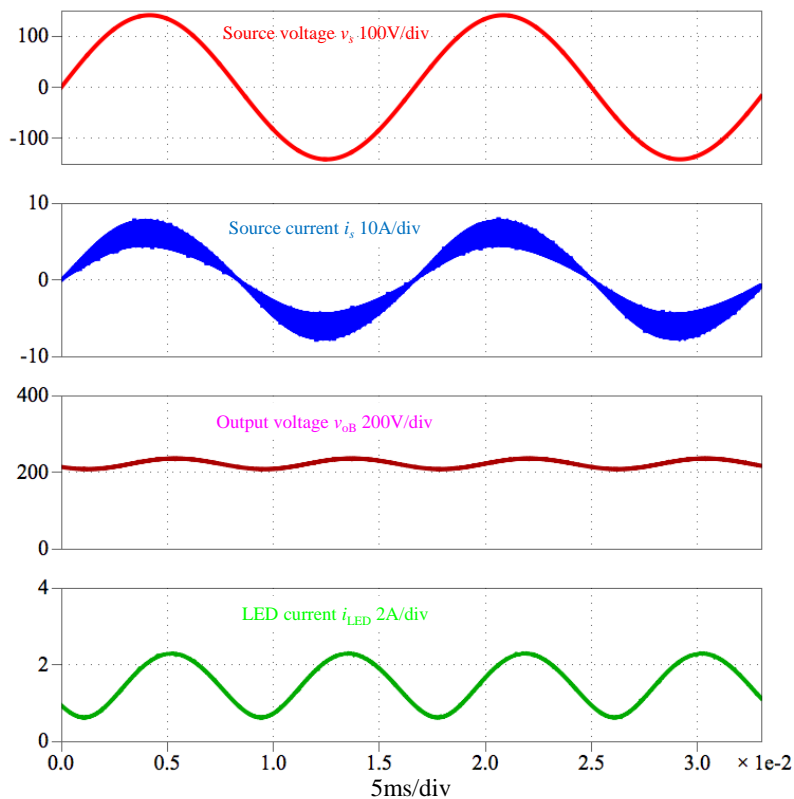


Figure 10. Simulation results of the proposed cooperative control method when the reference LED current I_{LED}^* is 1.5 A.

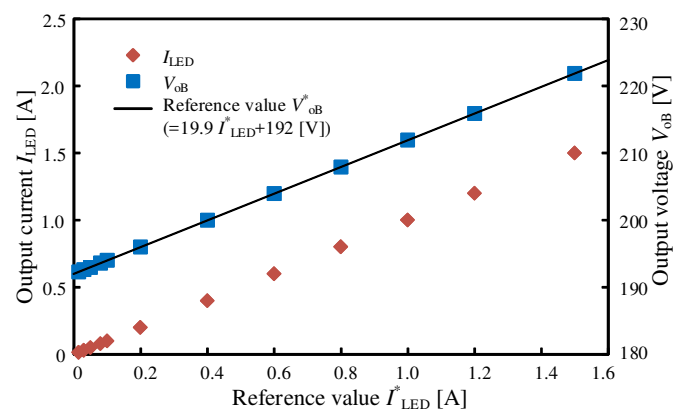


Figure 11. Simulation results of the output current I_{LED} and voltage V_{oB} for the reference LED current I_{LED}^* .

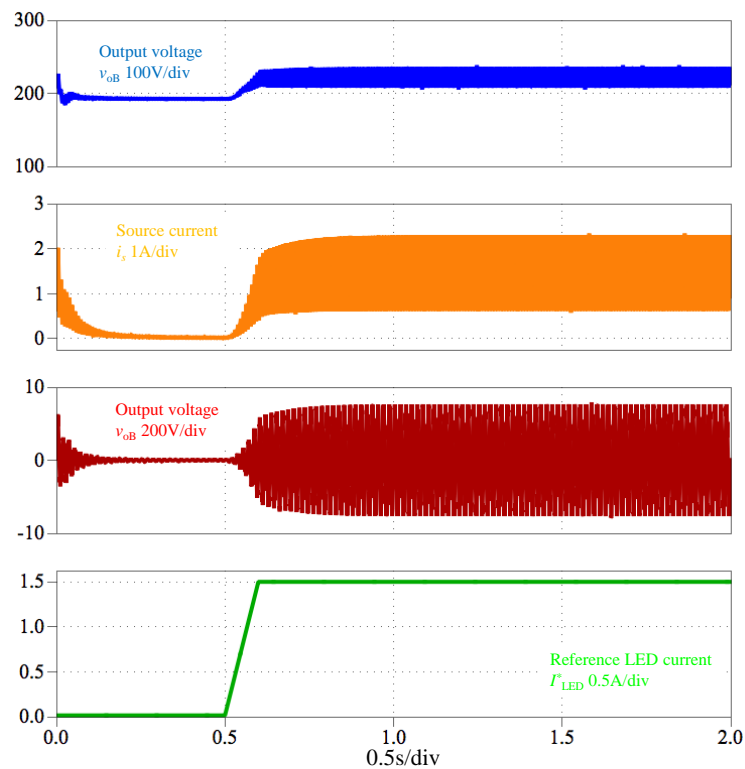


Figure 12. Simulation waveforms when the reference LED current I_{LED}^* is changed from 15 mA to 1.5 A.

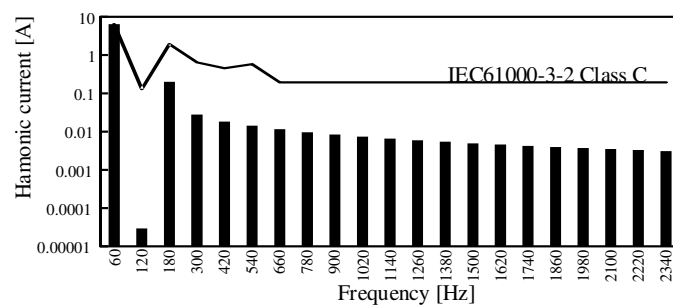


Figure 13. Fast Fourier Transform (FFT) analysis result when the average LED current is 1.5 A.

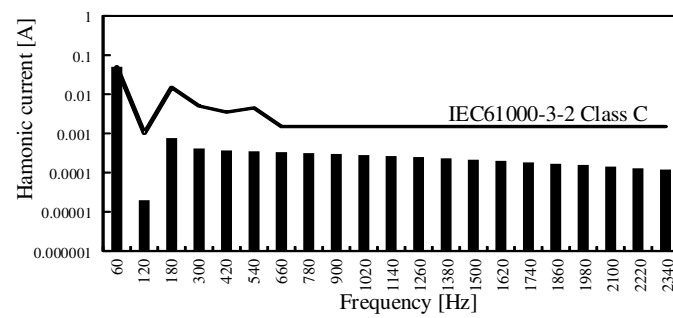


Figure 14. FFT analysis result when the average LED current is 15 mA.

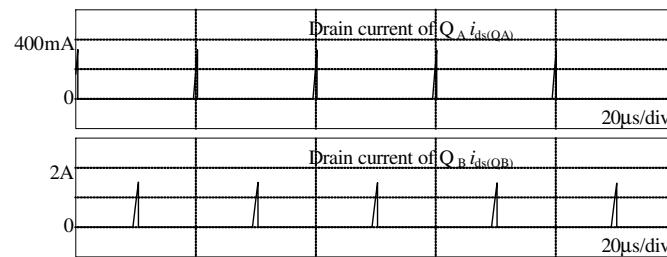


Figure 15. Simulation results of the proposed cooperative control method when the reference LED current I_{LED}^* is 15 mA.

6. Experimental Results

A prototype LED driver with the proposed cooperative control method was constructed and tested. A digital controller (TMDSDOCK28035) (Texas Instruments Incorporated, Dallas, TX, USA) including a digital signal processor (DSP: TMS320F28035, 60 MHz) (Texas Instruments Incorporated, Dallas, TX, USA) was used in the experimental setup. Figure 16 shows the picture of the LED driver used in an experiment.

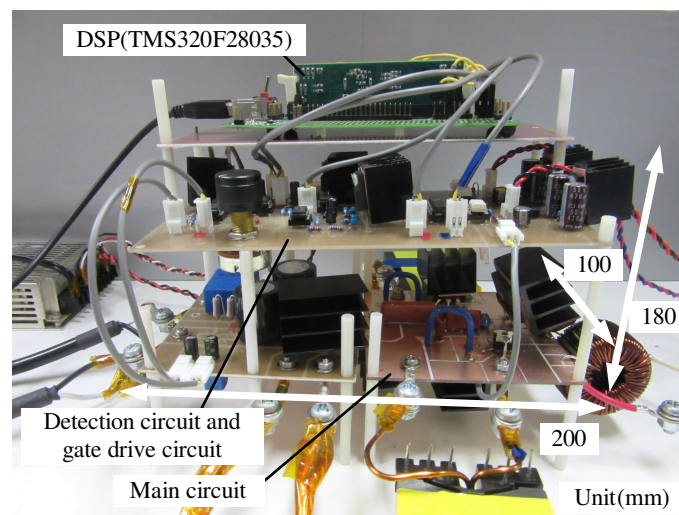


Figure 16. The picture of the LED driver used in an experiment.

Figures 17 and 18 show the experimental results of the proposed cooperative control method when the reference LED current I_{LED}^* is 1.5 A and 15 mA. v_s is the source voltage, i_s is the source current, V_{OB} is the output voltage of the buck–boost chopper, and I_{LED} is the LED current. From Figure 17, i_s is observed to be nearly sinusoidal and the power factor is 0.99. The average LED current

agrees with the reference LED current of 1.5 A. Although the LED current fluctuates by twice the source frequency, the LED current is always above over 5% of the rated LED current. This means that the proposed LED driver satisfies the standard of the Electrical Appliances and Materials Safety Act in Japan.

Figures 19 and 20 show the FFT analysis results of i_s . From these figures, it can be inferred that the LED driver with the proposed cooperative control method can satisfy the conditions in IEC61000-3-2.

Figure 21 shows the LED current and the output voltage of the buck–boost chopper for the reference output current I_{LED}^* . In Figure 21, the red and blue dots represent the experimental results. From Figure 21, we can see that the outputs of both converters agree with the reference values.

Figure 22 shows the experimental results of the drain currents $v_{D(QA)}$ and $v_{D(QB)}$ at a reference LED current I_{LED}^* 15 mA. From these waveforms, it can be observed that the on-intervals $T_{on(QA)}$ and $T_{on(QB)}$ are always more than 300 ns.

Figure 23 shows the experimental result when the reference LED current I_{LED}^* is changed from 15 mA to 1.5 A. In Figure 23, the green line is the reference voltage given for the analog channel of the DSP. When this value is 3 V, the I_{LED}^* is 1.5 A. From this result, I_{LED} agrees with I_{LED}^* .

Figure 24 shows the comparison of illuminance between minimum and maximum LED currents. The proposed LED driver doesn't cause flicker for all dimming region.

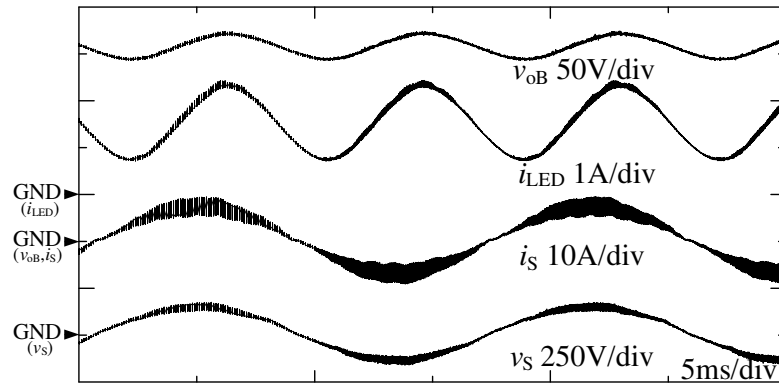


Figure 17. Experimental results of the proposed cooperative control method when the reference LED current I_{LED}^* is 1.5 A.

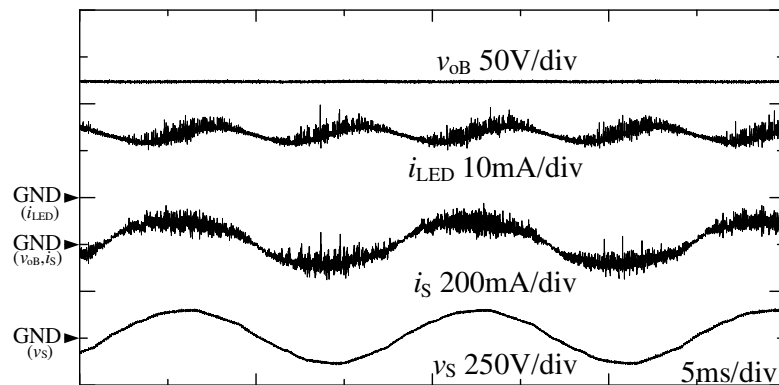


Figure 18. Experimental results of the proposed cooperative control method when the reference LED current I_{LED}^* is 15 mA.

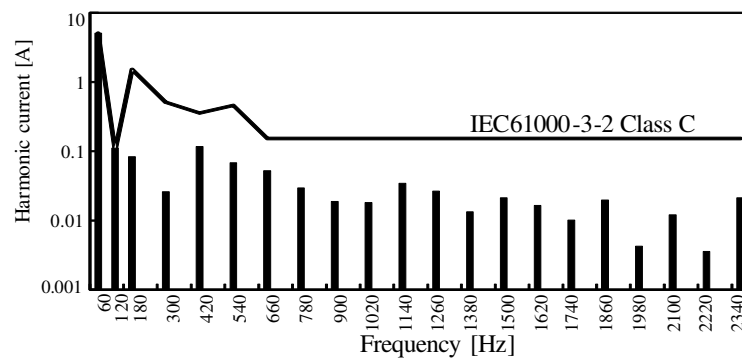


Figure 19. FFT analysis result when the average LED current is 1.5 A.

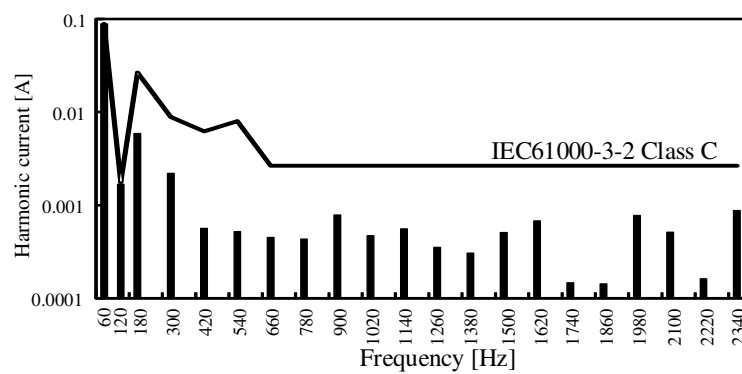


Figure 20. FFT analysis result when the average LED current is 15 mA.

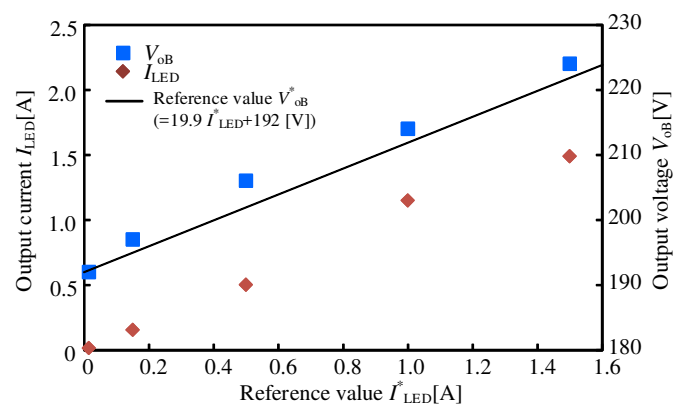


Figure 21. Experimental results of the output current I_{LED} and voltage V_{oB} for the reference LED current I_{LED}^* .

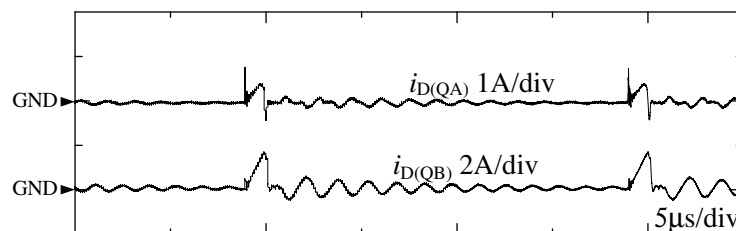


Figure 22. Experimental results of the proposed cooperative control method when the reference LED current I_{LED}^* is 15 mA.

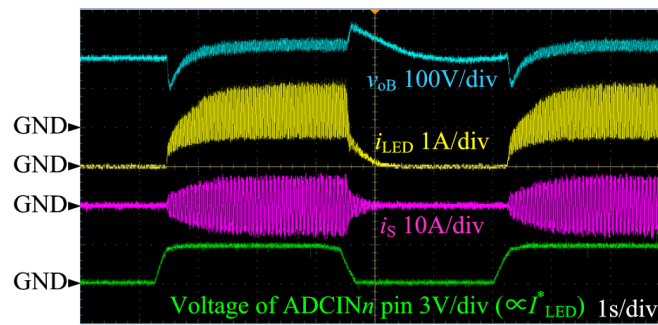


Figure 23. Experimental result when the reference LED current I_{LED}^* is changed from 15 mA to 1.5 A.

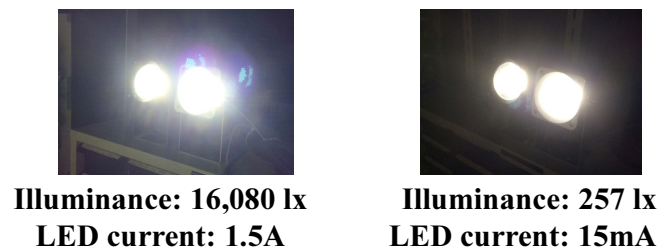


Figure 24. Comparison of illuminance between minimum and maximum LED currents.

7. Comparison of Power Conversion Efficiency between Si- and SiC-MOSFETs

Now, we discuss the power conversion efficiency. Figure 25 shows loss analysis of the experimental circuit when the output current is 1.5 A. The power conversion efficiency is 90.5%, and the total loss is 45.4 W. The losses of the MOSFETs Q_A and Q_B are dominated by the conduction losses when the output power is high. When the output current is 1.5 A, the conduction losses of Q_A and Q_B are 3.0 W and 3.3 W, respectively. The losses in MOSFETs are 10.1 W, which is 22.2% of the total loss. Thus, it is verified that reducing the conduction losses helps improve the power conversion efficiency of the experimental circuit.

SiC offers a low on-state resistance for purposes reducing the conduction loss. We use the SiC-MOSFETs C3M0065090J and C2M0040120D for Q_A and Q_B , respectively.

Table 2 shows Si- and SiC-MOSFET Parameters in the experimental setup. From Table 2, the drain-source on-state resistance of Q_A and Q_B are reduced about 77% and 40% by replacing Si-MOSFETs with SiC-MOSFETs.

Figure 26 shows loss analysis of the experimental circuit when the output current is 1.5 A. When the output current was 1.5 A, the conduction losses of Q_A and Q_B are 0.76 W and 1.15 W, respectively. The conduction losses are reduced by 74.8% and 42.8%, respectively. By replacing the Si-MOSFETs with SiC-MOSFETs, the power conversion efficiency was improved by 0.9%. Figure 27 shows experimental results of the power conversion efficiency. From this result, the power conversion efficiency of the SiC-MOSFETs-based proposed LED driver is higher than that of the Si-MOSFETs-based proposed LED driver over the whole region.

Table 3 shows the comparison result between the conventional and proposed methods. The proposed LED driver was tested for the source voltage 100 Vrms. However, the SiC-MOSFETs based LED driver can connect to the source voltage 300 Vrms. The proposed LED driver can control LED current linearly. In the proposed method with Si-MOSFET, the efficiency is over 90% in the range of 34% or more rated current. In the proposed method with SiC-MOSFET, the efficiency is over 90% in the range of 17% or more rated current.

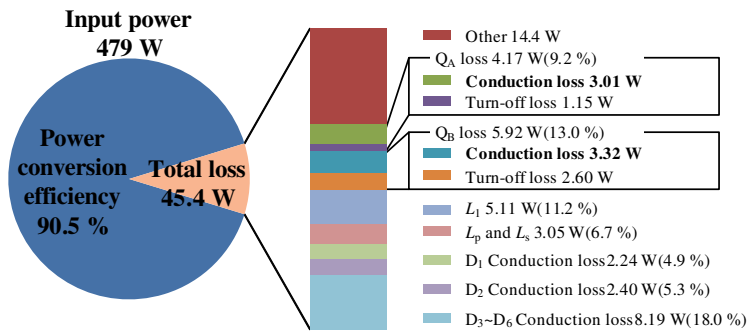


Figure 25. Loss analysis of the LED driver using Si MOSFET DC-DC converters.

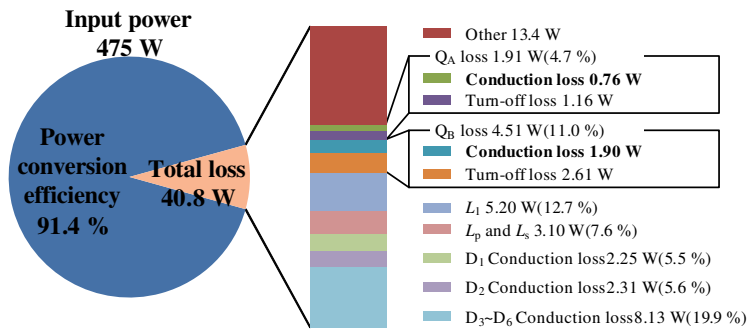


Figure 26. Loss analysis of the LED driver using SiC MOSFET DC-DC converters.

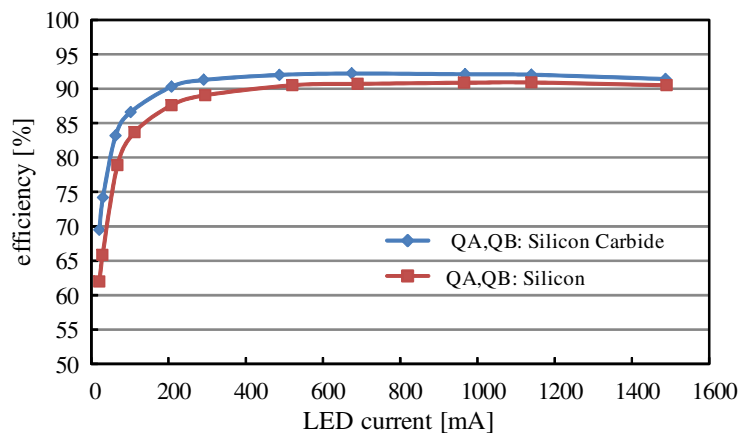


Figure 27. Experimental results of the efficiency for the output current I_{LED} .

We discuss about the heat sink of the MOSFET Q_A and Q_B .

The thermal resistance of the heat sink Rth_{h-a} can be expressed by:

$$Rth_{h-a} = \frac{T_j - T_a}{P_{loss}} - Rth_{j-p} - Rth_{p-h}, \quad (15)$$

where T_j is the device junction temperature, T_a is ambient temperature, P_{loss} is the loss of the MOSFET, Rth_{j-p} is the thermal resistance from the device junction to the package surface and Rth_{p-h} is the thermal resistance from the package surface to the heat sink.

Figure 28 shows the outline drawing of the heat sink that has six fins. The width and length of the heat sink are determined according to the TO-220 package size. The surface area of the heat sink S_h can be expressed by:

$$S_h = 6 \times 2 \times 0.025 \times H \times 10^{-3}. \quad (16)$$

In addition, Rth_{h-a} can be expressed with S_h by:

$$Rth_{h-a} = \frac{1}{hS_h}, \quad (17)$$

where h is the heat transfer coefficient of the heat sink. To estimate the height of the heat sink H , it is assumed that Rth_{j-p} is $5^\circ\text{C}/\text{W}$ and Rth_{p-h} is $1^\circ\text{C}/\text{W}$, h is $5\text{ W}/\text{m}^2\text{ }^\circ\text{C}$. From Equations (15)–(17), if T_j is 150°C and T_a is 50°C , H can be expressed by:

$$H = \frac{10^3}{1.5 \left(\frac{100}{P_{\text{loss}}} - 6 \right)}. \quad (18)$$

Table 2. Si- and SiC-metal-oxide-semiconductor field-effect transistors (MOSFETs) parameters in the experimental setup.

Parameter	Q_A		Q_B	
	(SiC-MOSFET)	(Si-MOSFET)	(SiC-MOSFET)	(Si-MOSFET)
	C3M0065090J	STF20NM65N	C2M0040120D	TK40J60T
Drain-source voltage V_{DS} (V)	900	650	1200	600
Gate-source voltage V_{GS} (V)	−8/19	−25/25	−10/25	−30/30
Continuous drain current (A)	$T_C = 25^\circ\text{C}$	35	15	40
	$T_C = 100^\circ\text{C}$	22	9.45	60
Junction temperature T_j ($^\circ\text{C}$)	−55 to 150	−55 to 150	−55 to 150	−55 to 150
Drain-source on-state resistance ($\text{m}\Omega$)	$T_C = 25^\circ\text{C}$	65	250	40
	$T_C = 100^\circ\text{C}$	78	270	52
Input capacitance C_{iss} (pF)	660	1280	1893	3900
Output capacitance C_{oss} (pF)	60	110	150	9200
Reverse capacitance C_{rss} (pF)	4.0	10	10	280

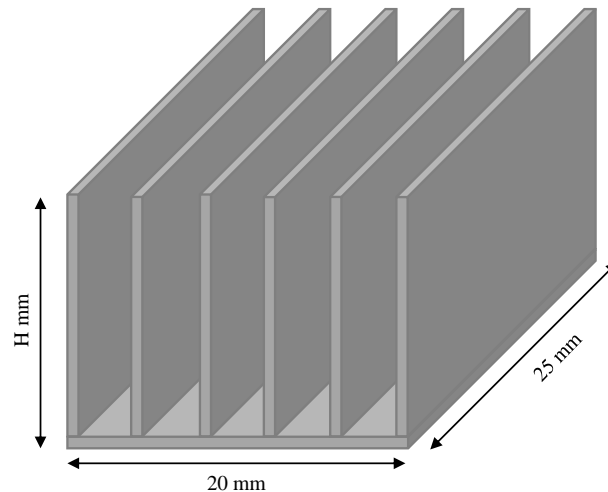
Table 3. Comparison between the conventional and proposed methods.

Item	Conventional Method	Proposed Method with Si-MOSFETs	Proposed Method with SiC-MOSFETs
AC input voltage	185–265 Vrms	100 Vrms	100 Vrms
Output power	210 W	408 W	408 W
Dimming type	Step	Linear	Linear
Dimming range (%)	50, 75, 100	1–100	1–100
Efficiency at maximum output power	92.1%	90.5%	91.4%
Efficiency at minimum output power	90.7%	62.0%	69.5%
Minimum illuminance of LEDs	1680lx	257lx	257lx

Table 4 shows the estimation of the heat sink size. From Table 4, the heat sink volume of Q_A and Q_B is reduced 61% and 32% by replacing the Si MOSFET with SiC MOSFET. In this paper, all converters are driven in the discontinuous mode (DCM). However, in order to further improve the efficiency, it is also possible to consider critical conduction mode (CRM).

Table 4. Estimation of the heat sink size.

Item	Q_A		Q_B	
	Si-MOSFET	SiC-MOSFET	Si-MOSFET	SiC-MOSFET
Loss	4.17 W	1.91 W	5.92 W	4.51 W
Height of the heat sink	37 mm	14.4 mm	61.2 mm	41.2 mm

**Figure 28.** Outline drawing of the heat sink.

8. Improvement of Power Conversion Efficiency for Low LED Current Region

The power conversion efficiency of the proposed LED driver is low for the low LED current region. The loss of the MOSFET Q_B is dominated by the turn-off loss when the output power is low. In addition, the turn-off loss of Q_B can be expressed by:

$$P_{s_Q_B} = f_{sw} \int_{t_0}^{t_0 + \Delta T_{off}} v_{DS(Q_B)} i_{D(Q_B)} dt, \quad (19)$$

where f_{sw} is the switching frequency, t_0 is the start time of Q_B turn-off period and ΔT_{off} is the Q_B turn-off period. From Equation (19), the turn-off loss depends on the switching frequency and the turn-off loss is reduced by lowering the switching frequency.

Figure 29 shows a control block of the proposed cooperative control method with variable switching frequency. We added the variable switching frequency function to the proposed control block. This function has hysteresis characteristics with I_{LED}^* . Figure 30 shows the relationship between the LED reference current and the switching frequency. In addition, the hysteresis characteristics can be expressed by:

$$\begin{cases} I_{LED}^* \geq I_{(upper\ limit)} \rightarrow f_{sw} = 50 \text{ kHz}, \\ I_{LED}^* \leq I_{(lower\ limit)} \rightarrow f_{sw} = 25 \text{ kHz}. \end{cases} \quad (20)$$

We determined $I_{(upper\ limit)}$ and $I_{(lower\ limit)}$ by comparing the experimental result of the efficiency with the switching frequency as 25 kHz and 50 kHz.

Figure 31 shows the experimental result of the efficiency with the switching frequency as 25 kHz and 50 kHz. In Figure 31, Si MOSFETs are used for the proposed LED driver. When the output current is smaller than 250 mA, the power conversion efficiency of the switching frequency 25 kHz is higher than that of the switching frequency 50 kHz. Therefore, we decided that $I_{(upper\ limit)}$ is 300 mA and $I_{(lower\ limit)}$ is 200 mA. As a result, when the output current is 15 mA, the power conversion efficiency is improved by about 5%.

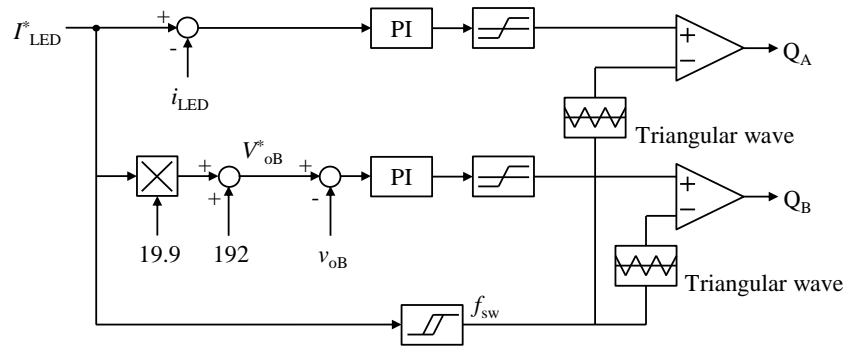


Figure 29. Control block of the proposed cooperative control method with variable switching frequency.

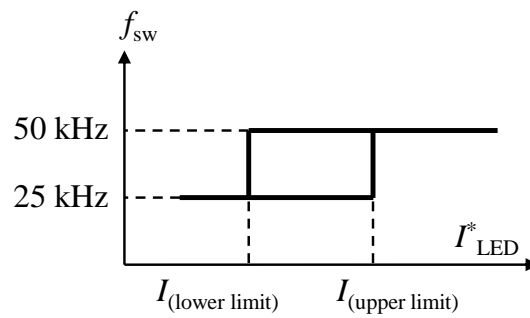


Figure 30. Relationship between the LED reference current and the switching frequency.

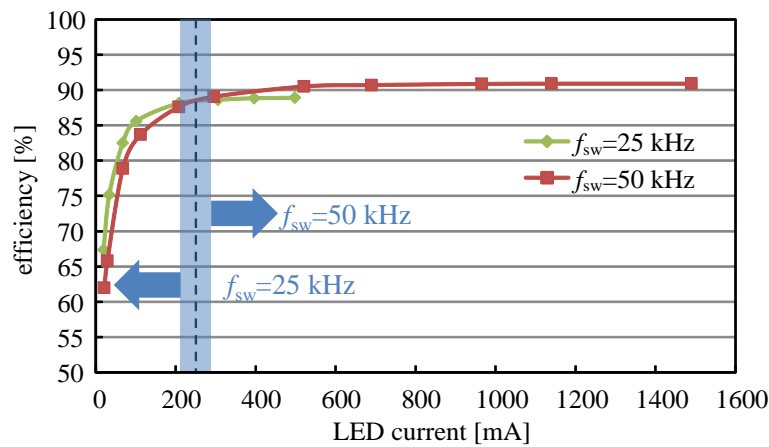


Figure 31. Experimental results of the efficiency with the switching frequency as 25 kHz and 50 kHz.

9. Conclusions

This paper described the design and experimental verification of 400-W class LED driver with cooperative control method for two-parallel connected DC/DC converters. This proposed cooperative control method drove two DC/DC converters, based on the reference LED current. All converters operated in the DCM to improve the power factor using simple controllers. In this paper, the circuit parameters were designed for DCM and for the stable on-intervals of switching devices. A prototype LED driver using the proposed cooperative control method was built and tested. From the simulation and experimental results, the on-intervals of the MOSFETs were observed to be higher than 300 ns under dimming operation from 1% to 100%, by using the cooperative control method. The proposed LED driver reduced the minimum LED current by 90.7%, compared to the conventional control method. From simulation and experimental results, the linear dimming of the proposed LED driver achieved stable operation when the reference LED current was changed from 1% to 100%. The maximum power

conversion efficiency by using SiC-MOSFETs based LED driver is 91.4%. Finally, the variable switching frequency method is proposed for improving the power conversion efficiency for low LED current region. Experimental results revealed that the power conversion efficiency can be improved for the low LED current region. Dynamic analysis was not conducted in this paper. In a future work, it would be important to examine the system for its stability.

Author Contributions: T.Y. significantly contributed to the design of the proposed LED driver and the implementation of the computer simulation. Y.K. contributed the fabrication of the experimental setup and its evaluation. H.Y. proposed the basic control topology and helped with the writing of this paper. T.T., M.O. and T.H. were responsible for guidance and key suggestions.

Funding: This research received no external funding.

Conflicts of Interest: The authors declare no conflict of interest.

Abbreviations

The following abbreviations are used in this manuscript:

LED	Light-emitting diode
DCM	Discontinuous conduction mode
THD	Total harmonic distortion
MOSFET	Metal-oxide-semiconductor field-effect transistor
PFC	Power factor correction
FFT	Fast Fourier Transform
DSP	Digital signal processor

References

1. International Energy Agency. Energy Matters. Available online: <https://www.iea.org/publications/freepublications/publication/EnergyMattersBrochure.2.pdf> (accessed on 25 July 2016).
2. United Nations Environment. Minamata Convention on Mercury. Available online: <http://www.unep.org/hazardoussubstances/Portals/9/Mercury/Documents/dipcon/CONF3Minamata%20Convention%20on%20Mercuryfinal%2026%2008e.pdf> (accessed on 25 July 2016).
3. Schratz, M.; Gupta, C.; Struhs, T.J.; Gray, K. Improving light quality with cost-effective LED technology. *IEEE Ind. Appl. Mag.* **2016**, *22*, 55–62. [CrossRef]
4. Lee, J.-Y.; Moon, G.-W.; Park, H.-J.; Youn, M.-J. Integrated ZCS Quasi-Resonant Power Factor Correction Converter Based on Flyback Topology. *IEEE Trans. Power Electron.* **2000**, *15*, 634–643.
5. Arias, M.; Lamar, D.G.; Linera, F.F.; Balocco, D.; Diallo, A.A.; Sebastian, J. Design of a Soft-Switching Asymmetrical Half-Bridge Converter as Second Stage of an LED Driver for Street Lighting Application. *IEEE Trans. Power Electron.* **2012**, *27*, 1608–1621. [CrossRef]
6. Xie, X.; Li, J.; Peng, K.; Xhao, C.; Lu, Q. Study on the Single-Stage Forward-Flyback PFC Converter with QR Control. *IEEE Trans. Power Electron.* **2016**, *31*, 430–442. [CrossRef]
7. Cheng, C.-A.; Cheng, H.-L.; Chung, T.-Y. A Novel Single-Stage High-Power-Factor LED Street-Lighting Driver With Coupled Inductors. *IEEE Trans. Ind. Appl.* **2014**, *50*, 3037–3045. [CrossRef]
8. Cheng, C.-A.; Chang, C.-H.; Chung, T.-Y.; Yang, F.-L. Design and Implementation of a Single-Stage Driver for Supplying an LED Street-Lighting Module With Power Factor Corrections. *IEEE Trans. Power Electron.* **2015**, *30*, 956–966. [CrossRef]
9. Moo, C.-S.; Chen, Y.-J.; Yang, W.-C. An Efficient Driver for Dimmable LED Lighting. *IEEE Trans. Power Electron.* **2012**, *27*, 4613–4618. [CrossRef]
10. Jane, G.; Su, C.-C.; Chiu, H.-J.; Lo, Y.-K. High-Efficiency LED Driver for Street Light Applications. In Proceedings of the International Conference on Renewable Energy Research and Applications (ICRERA), Nagasaki, Japan, 11–14 November 2012; pp. 105–107.
11. Yada, T.; Yamada, H.; Hanamoto, T. A Novel Cooperational Control Method for LED Driver with Parallel Flyback Converter. *J. Jpn. Inst. Power Electron.* **2015**, *40*, JIPE-40-19.

12. Katamoto, Y.; Yamada, H.; Tanaka, T.; Okamoto, M.; Yada, T. Experimental Verification of Cooperative Control Method for 400-W Class LED Drivfer With Wide Dimming Range. In Proceedings of the 19th International Conference on Electrical Machines and Systems, Chiba, Japan, 13–16 November 2016; p. DS4G-2-8.
13. Ministry of Economy, Trade, and Industry. *Electrical Appliances and Materials Safety Act*; Ministry of Economy, Trade and Industry: Chiyoda, Japan, 2018.



© 2018 by the authors. Licensee MDPI, Basel, Switzerland. This article is an open access article distributed under the terms and conditions of the Creative Commons Attribution (CC BY) license (<http://creativecommons.org/licenses/by/4.0/>).